

DIAGNOSTICS OF ACTUATION SYSTEMS FAULTS FROM DYNAMIC DATA

Pier Carlo Berri¹, Matteo D. L. Dalla Vedova¹ and Laura Mainini^{1,2}

¹ Department of Mechanical and Aerospace Engineering, Politecnico di Torino
Corso Duca Degli Abruzzi, 24, 10129 Torino TO (Italy)
{pier.berri,matteo.dallavedova,laura.mainini}@polito.it

² Department of Aeronautics and Astronautics, Massachusetts Institute of Technology
77 Massachusetts Avenue, Cambridge, MA, 02139 (USA)

Key words: Reduced-Order Model, Proper Orthogonal Decomposition, Self-Organizing Maps, Dynamic Data, Actuator Diagnostics

Abstract. For aircraft actuation systems, the use of an online diagnostic tool to detect the system damages at their early stages could be exploited to optimize the condition-based maintenance planning, with improvements in safety and operating costs. This paper proposes a computational strategy for the online diagnostics of actuation systems faults, combining an optimal sampling strategy with different approaches for parameter identification and exploiting the information gathered from different numerical models of the system to estimate its health status. The method leverages low dimensional representations of the quantity to monitor using a signal compression method, based on Proper Orthogonal Decomposition and Self-Organizing Maps, to speed up the solution of the parameter identification problem with the limited hardware resources available onboard. The method is tested for the fault detection of an electromechanical actuator for aircraft flight control systems.

1 INTRODUCTION

The growing complexity of current and next generation aircraft systems is progressively increasing the maintenance-related costs. The traditional approach, based on *a priori* scheduling of maintenance intervention, has to face the great variety of failure modes related to the large number of heterogeneous subsystems and components on board the vehicles, resulting in a poorly accurate and highly inefficient estimation of the system useful life. Great improvement would be achieved by implementing methods and strategies for the continuous evaluation of the Remaining Useful Life (RUL) of components, based on their current health condition. This way, the substitution of Line Replaceable Units (LRUs) could be scheduled with great accuracy and the mission profile of the aircraft could be adapted to its health status, to avoid overstressing components, reduce the costs associated with maintenance, and increase safety [1, 2].

The first step necessary for a precise system RUL estimation consists in the Fault Detection and Identification (FDI) phase, aimed at the acquisition of the system health status with the highest possible accuracy, detecting faults in their early stages, before they start affecting the system performance [3]. Traditional FDI algorithms imply the acquisition, storage and processing of significant amount of data, which is not compatible with the real time execution needed for a continuous RUL estimation. Moreover, this task shall be executed on the limited hardware resources available on board, which lack both the amount of memory needed to store the measured data and the processing power necessary to identify a fault in a useful time.

In this paper, we propose a methodology to perform an accurate and computationally efficient FDI for a dynamical system. This strategy relies on a multifidelity approach, combining the information acquired through different models of the system, with a different level of complexity, employed in different phases of the procedure. During the offline phase, a High Fidelity (HF) model is employed to compute the reference data and learn about the system behavior in different faulty conditions. Then, Proper Orthogonal Decomposition (POD) [4, 5, 6] and Self Organizing Maps (SOM) [7, 8, 9] are combined to identify an optimal placement of sampling points, and to obtain an informative compressed representation of the quantities to measure and monitor online. The online phase consists in a standard parameter identification problem, in which the inputs of a Low Fidelity (LF) model are adjusted to match the response of the physical system. In particular, we consider two different LF representations of the system, namely a simplified dynamic model of the actuation system to monitor (LF1) and a library-based emulator of the signal to measure (LF2).

The purpose of this work is to obtain and process a compressed representation of the signal to monitor in order to reduce the dimensionality of the parameter identification problem online. The aforementioned optimal sampling technique is combined with different methods for the parameter identification problem, to assess the performances in terms of accuracy and computational time. We adopt the proposed methodology to address the FDI problem for an electromechanical actuation system of an aircraft flight control system, affected by multiple mechanical and electrical damages.

2 PROBLEM SETUP

Electromechanical Actuators (EMAs) are a class of actuation systems which exploit electrical power to control the position of a mechanical component, such as an aircraft flight control surface, referred to as the *user*. Their architecture is usually composed by an electric motor driving the user through a high gear ratio mechanical gear-box; the user position is measured by a sensor, consisting in either a potentiometer, a Linear Variable Differential Transformer (LVDT), or an optical encoder, and fed back to the control electronics, which determines the voltage applied to the motors according to the difference between commanded and actual user position.

The use of EMAs in place of the more traditional hydraulic actuator is gradually spreading in a number of airborne applications, ranging from the primary flight control system of small to medium Unmanned Aerial Vehicles, to secondary and backup functions on larger

aircraft. The implementation of these systems can lead to an overall weight reduction at aircraft level [10], eliminating the need of a centralized hydraulic system; on the other hand, the presence of a complex mechanical transmission between the motor and the final user (i.e. aerodynamic surface) introduces the risk of mechanical jamming as a potential failure mode, which is virtually impossible for hydraulic systems. This eventuality leads to the impossibility to control the aircraft, which can result in catastrophic accidents. For this reason, an active and continuous health monitoring is important to enable the use of EMAs on flight critical functions without reducing the system safety.

We consider an EMA for the flight control system of a light aircraft consisting in a three phase brushless motor, a four stages epicycloidal gear-box, an LVDT as the user position transducer and a control and power electronics board. We face the problem of detecting the health status of the EMA, as a set of parameters which represent the most common fault modes [11]. Those faults are chosen for their relatively high rate of occurrence, among the ones characterized by a slow and progressive growth. The levels of severity of each damage is encoded in the variation from the nominal (without faults) value of one element of the fault vector $\mathbf{k} = [k_1, \dots, k_6]$, which components are: dry friction acting on the mechanical transmission (k_1), backlash of the transmission (k_2), partial phase short circuit (k_3, k_4, k_5 for the three motor phases A, B and C), static eccentricity of the rotor (k_6). Each element of \mathbf{k} is normalized with the value corresponding to a complete failure of the electromechanical actuators.

The variable to monitor is a current signal $\mathbf{i}(\mathbf{k})$ defined as the envelope of the three phase currents of the brushless motor. Two reasons motivate this choice: (1) the sensitivity of this quantity to the variation of the fault vector is much greater than the other available variables; (2) the motor currents are already measured for feedback and control purposes, so the diagnostic function does not need additional hardware in terms of sensors and transducers. For the analysis performed in this work, three models of the same EMA are considered, each characterized by different levels of complexity and fidelity, namely a HF dynamical model, a simplified LF dynamical model and a second LF model consisting in a library based signal emulator. Each model reproduces the dynamical response of the actuator in terms of motor current with different accuracy and at different computational costs.

2.1 High Fidelity Model (HF)

The HF representation of the EMA simulates with great detail the physical phenomena underlying the system behavior, at the expense of a rather long computational time. The EMA is represented with a Simulink model: the different constitutive blocks simulate the physics of the components of the EMA. The model accounts for different noise sources and higher order effects, including: the analog to digital conversion of the controller signals, the Pulse Width Modulation (PWM) hysteresis control of the three motor phase currents, the effects of the electromagnetic couplings between the motor stator and rotor affecting the generated torque and the counter electromotive force, and the mechanical nonlinear effects of static and dynamic friction, backlash and end-of-travels.

This HF model is the representation of the system that we use as primary source of

reference data, and its computational time ranges from tenths of seconds to a few minutes when executed on a common laptop of medium performances for the simulation of a 0.5s response. A detailed description of the HF model can be found in [12].

2.2 First Low Fidelity Model (LF1)

The first LF model (LF1) is a simplified dynamical model of the EMA, representing the behavior of complex subsystems with simpler blocks. The main simplification in the LF1 model is the elimination of the three phase electromechanical model of the brushless motor, which accounts for most the complexity and computational resources required by the HF model. The electromechanical model is then replaced by an equivalent single phase DC motor model, which parameters are tuned to give the same overall performances (in terms of torque, power and counter electromotive force coefficient) of the brushless motor in the HF model. Another difference between the HF and LF1 models is the absence, in the latter, of the PWM hysteresis control of the motor current, replaced by a sign block and a proportional gain, which allows for a stable numerical integration with longer time steps compared to what required for the HF model.

As a result, the integration time step can be increased by an order of magnitude without incurring in numerical instability problems, and the evaluation time of each step is greatly reduced; this way, the model is more efficient computationally, with improvements of more than one order of magnitude with respect to the HF model. A more detailed description of the LF1 model can be found in [12].

2.3 Second Low Fidelity Model (LF2)

The second Low Fidelity model (LF2) is implemented as a non-dynamical physics-based simulation, in order to further reduce the computational time. This model acts as a signal emulator: it computes the system output as the combination of a library of pre-computed outputs from the HF model, as a function of the fault parameters vector, rather than through the integration of a dynamical system. This operation is possible by assuming that the effects of different faults are separable with a negligible loss of accuracy, that is when the combined effect of multiple faults is much smaller than the effects of the same faults considered alone.

The LF2 output is obtained by adding the perturbations produced by the fault parameters to the nominal condition current signal, computed offline with the HF model and saved. Each perturbation is computed separately by adding a pre-stored signal weighted with the corresponding fault parameter or with the nominal current value:

$$\mathbf{i}(\mathbf{k}) = (\mathbf{i}_0 + \mathbf{i}_{\text{SF}}f_1(k_1) + \mathbf{i}_{\text{BLK}}(k_2)) \left(1 + \mathbf{i}_\zeta(k_6) + \sum_{j=3}^5 \mathbf{i}_{\text{PHA,B,C}}f_2(k_j) \right) \quad (1)$$

In equation (1) \mathbf{i}_0 is the current in nominal conditions, $\mathbf{i}_{\text{SF}}f_1(k_1)$ is the disturbance produced by static friction, $\mathbf{i}_{\text{BLK}}(k_2)$ is the disturbance produced by backlash, $\mathbf{i}_\zeta(k_6)$ is the modulation produced by rotor static eccentricity and \mathbf{i}_{PHA} , \mathbf{i}_{PHB} , \mathbf{i}_{PHC} are the modulations produced by the partial short circuit of phases A, B and C respectively. The functions f_1

and f_2 are polynomial regressions optimized to reproduce the behavior of the reference system as accurately as possible.

The LF2 model greatly reduces the computational time of three orders of magnitude compared to the HF; however, it is the least accurate (especially in presence of combinations of more than one fault mode) and is generated by a trial and error procedure. Then, the use of such approach is strongly problem-dependent and can be hardly generalized.

3 METHODOLOGY

Detecting the faults of a dynamical system is a parameter identification problem. The response of the system in terms of one or more time dependent quantities is acquired through a given set of sampling points and is compared with that obtained through a computationally efficient LF model to estimate the damages affecting the system, which cause the discrepancy between the two responses.

The measured quantity, specifically the envelope current $\mathbf{i}(\mathbf{k})$, is sensitive to the effects of a number of fault modes. In the offline phase, the sampling points are determined to capture most of the signal information with a compressed representation. Then, in the online phase, the fault parameters are estimated by processing the compressed current signal.

3.1 Signal compression strategy (offline)

The use of traditional techniques to perform the parameter estimation would require a large amount of computational power and storage capability to convey a sufficient amount of information from the system output through the following steps of the identification algorithm. This is due to the complexity of physical phenomena underlying the system and the high dimensionality of the problem. Then, an efficient signal compression is needed to reduce the amount of data to store and process, enabling the evaluation of the fault parameters with the available hardware resources.

The sampling technique exploits a two-step signal compression strategy that combines reduced order modeling (Proper Orthogonal Decomposition) and unsupervised competitive learning (Self-Organizing Maps) techniques to identify the most informative instants of time to be stored online for a single signal. POD is frequently used to compress and reconstruct high dimensional quantities [13, 14, 15, 16, 17]; in addition, a variety of compressive sensing techniques can be adopted to reconstruct measured quantities and signals [18, 19, 20, 21, 22]. In this work, the compression is not performed with the purpose of reconstructing the original signal, but to reduce storage and computational effort needed for the online execution of a fault detection algorithm. A first implementation of this method is proposed by [7].

Proper Orthogonal Decomposition The first step of the compression strategy uses Proper Orthogonal Decomposition (POD) [4, 23, 24, 25, 16] to identify a low dimensional representation of the physics to monitor, that is, of the envelope current \mathbf{i} as a function of the fault condition \mathbf{k} . We use the method of snapshots proposed by Sirovich [24] and collect current signals (snapshots) computed with the HF model for n_s different fault

conditions and sampled with a constant frequency to obtain a vector of n_t elements. Then a $n_t \times n_s$ snapshot matrix is assembled and the POD modes computed through singular value decomposition. POD modes $\{\mathbf{v}_j\}_{j=1}^{n_s}$ constitute an orthonormal basis that is optimal in the least square sense; the basis vectors are ordered according to the fraction of variance explained by each mode and expressed by the associated eigenvalue λ_j . A generic current signal $\mathbf{i}(\mathbf{k})$ can be expressed as a linear combination of the POD basis vectors \mathbf{v}_j :

$$\mathbf{i}(\mathbf{k}) \approx \mathbf{i}_0 + \sum_{j=1}^r \mathbf{v}_j \alpha_j(\mathbf{k}) \quad (2)$$

where \mathbf{i}_0 is the reference signal in nominal condition and $\alpha_j(\mathbf{k})$ are the coefficients of the POD expansion. For the purposes of the optimal sampling strategy for signal compression discussed in this paper, we are interested in the first $r \ll n_s$ POD modes that explain most of the information content captured by the snapshot matrix. In particular, the next step accounts only for the first dominant mode \mathbf{v}_1 .

Self-Organizing Maps The second step of signal compression uses Self-Organizing Maps (SOMs) [9, 26] to identify a set of highly informative sampling points that capture the information content of the first POD mode \mathbf{v}_1 . SOMs are single layer neural networks that use unsupervised competitive learning to compute models and identify underlying structures (e.g. clusters) of input data. The n_ω neurons of the SOM are represented in the input space as weight vectors $\{\boldsymbol{\omega}_j\}_{j=1}^{n_\omega}$ whose values are updated during network training. Once training is completed, the weight vectors identify centroids of n_ω distinct clusters of input data. In this work, SOM is trained with a data set $T = [\mathbf{v}_1, \mathbf{t}]$ constituted by the first POD mode \mathbf{v}_1 and the time coordinate \mathbf{t} . After training, the most informative time-locations of the sampling points are encoded in the time component (second element) of the $n_\omega \ll n_t$ weight vectors $\boldsymbol{\omega}_j = [\omega_{j1}, \omega_{j2}]$. Then, we can define a compressed EMA output signal $\hat{\mathbf{i}}(\mathbf{k})$ as the envelope current sampled at times $\boldsymbol{\omega}_2 = \{\omega_{j2}\}_{j=1}^{n_\omega}$.

3.2 Parameter identification (online)

In the online phase of the FDI procedure, parameter identification is achieved by minimizing the gap between measured compressed signal $\hat{\mathbf{i}}(\mathbf{k})$ and the signal estimate computed with a lower fidelity model. Different strategies among those commonly used for this class of problems are implemented and tested. The use of these methods for real time identification would be unpractical if complete signals $\mathbf{i}(\mathbf{k})$ were considered, for the high computational cost of processing high dimensional quantities.

Linearized parameter identification The first approach for parameter estimation is a linear direct identification, not requiring the online execution of a system model. If the variation of the system from the nominal condition is expected to be small, and if the system behavior is regular, we can assume the output signal to vary linearly with the components of the fault parameters vectors. Under those assumptions, the compressed current signal can be represented as:

$$\Delta \mathbf{i} = A \Delta \mathbf{k} \quad (3)$$

where $\Delta \mathbf{i} = \hat{\mathbf{i}} - \hat{\mathbf{i}}_0$ is the variation of the compressed current signal from the nominal condition and $\Delta \mathbf{k} = \mathbf{k} - \mathbf{k}_0$ is the variation of the fault parameters from the nominal condition. The matrix A is the system Jacobian evaluated in the reference condition \mathbf{k}_0 , whose j -th column contains the derivative of the reduced EMA output signal with respect to the j -th fault parameter, computed with a finite differences method.

Matrix A is computed offline and stored; online, the linear system (3) is solved to find $\Delta \mathbf{k}$ for measured $\Delta \mathbf{i}$: a least squares based estimate of the parameter vector \mathbf{k} is computed through QR factorization of matrix A in a single step. The signal compression allows to sensitively reduce the size of matrix A , which leads to a reduction of the computational effort to estimate \mathbf{k} . This method can provide reliable estimate for small values of the fault parameters (close to the nominal condition), where system behavior can be locally approximated with a linear model.

Iterative parameter identification with LF1 In order to perform a parameter identification in presence of large variations from the nominal condition highlighting the non-linear behavior of the system, one possible solution is to iteratively update the matrix A , linearizing the system behavior near the current estimated value of \mathbf{k} . In a few iterations the solution is expected to converge near the actual system health status. At each iteration j , the estimated \mathbf{k}_j and the Jacobian matrix $A(\mathbf{k}_j)$ (in short A_j) are updated:

$$\mathbf{k}_j = \mathbf{k}_{j-1} + C(A_j^\top A_j)^{-1} A_j^\top \Delta \mathbf{i}_j \quad (4)$$

where $\Delta \mathbf{i}_j = \hat{\mathbf{i}} - \hat{\mathbf{i}}_j$ and C is a factor to improve numerical stability. In order to avoid the inversion of the poorly conditioned $A^\top A$, a QR factorization is indeed employed to solve the least squares problem, as per the linearized direct identification.

In contrast with the previous method, now the QR factorization is computed online: the use of compressed signals $\hat{\mathbf{i}}$ permits to contain the size of matrix A and the computational burden associated with the solution of problem (4) at each iteration. However, the single estimate of A requires the execution of a system model; the use of the HF representation is computationally expensive and not viable for the online iterative computation. A possible solution is the use of the LF1 model to estimate both the iteration matrix A_j and the residual $\Delta \mathbf{i}$. With this approach, the system identification requires much more time than the non-iterative approach (even of some orders of magnitude), but it would be still compatible with a more traditional offline diagnostics.

Iterative parameter identification with LF2 An alternative version of the iterative method can use the LF2 model of the system for the online estimate of the matrix A at each iteration. The LF2 model provides a lower fidelity representation of system dynamics, but is computationally much less expensive than LF1.

4 RESULTS

The snapshot matrix assembles a reference dataset of $n_s = 5000$ signals, each consisting in the response to a chirp signal of small amplitude, computed with the HF model on a set of fault vectors sampled with a latin hypercube strategy. Each snapshot consists of a column vector of $n_t = 5001$ components, since the simulation of a 0.5s signal is sampled with a constant frequency of 10kHz. Then, we apply the two-step sampling strategy presented in Section 3.1. First, we compute the POD basis vectors and keep the first modal component \mathbf{v}_1 which alone explains approximately 75% of the information content of the reference dataset ($\lambda_1 / \sum_{j=1}^{n_s} \lambda_j = 0.7575$). Then, a $n_\omega = 30$ neurons SOM is trained over the set $T = [\mathbf{v}_1, \mathbf{t}]$ to identify 30 informative sampling points (Figure 1). The reduction from 5001 original signal points to 30 sample points allows to use standard methods for the subsequent parameter estimation problem, which would imply a prohibitive computational costs for online FDI whether applied to the full signal.

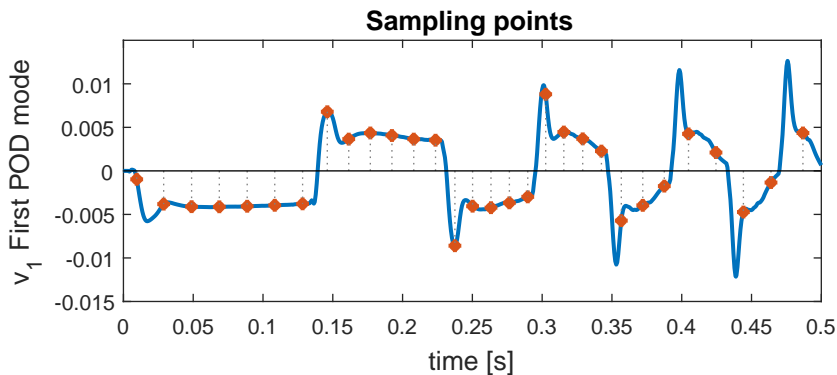


Figure 1: Time-locations of the $n_\omega = 30$ sampling points over the first POD mode \mathbf{v}_1

To assess the three parameter identification methods, two different test sets are computed with the HF model. Each test set includes 100 signals, corresponding to 100 fault conditions randomly sampled with a constant distribution limited to different ranges. Specifically, the first test set considers only small values for the fault parameters, so both the linearized and the iterative approaches are applicable; in the other test set, the variation from the nominal condition is larger, to assess the greater robustness of the iterative methods. However, the main purpose of the proposed FDI strategy is the identification of the early signs of system damages (which are better represented by the first test set) before they start compromising the EMA performances.

Figure 2 compares the performances of the three considered parameter estimation methods in combination with the optimal sampling, on the two test sets. Figure 2(left) shows the relative error on the parameter estimation problem, computed as:

$$err_k = \frac{\|\mathbf{k}\|}{\sqrt{6}} \quad (5)$$

Similarly, Figure 2(right) shows the error on the reconstructed signal $\hat{\mathbf{i}}$ as obtained with the low fidelity model used case by case (LF1 or LF2); the signal is reconstructed

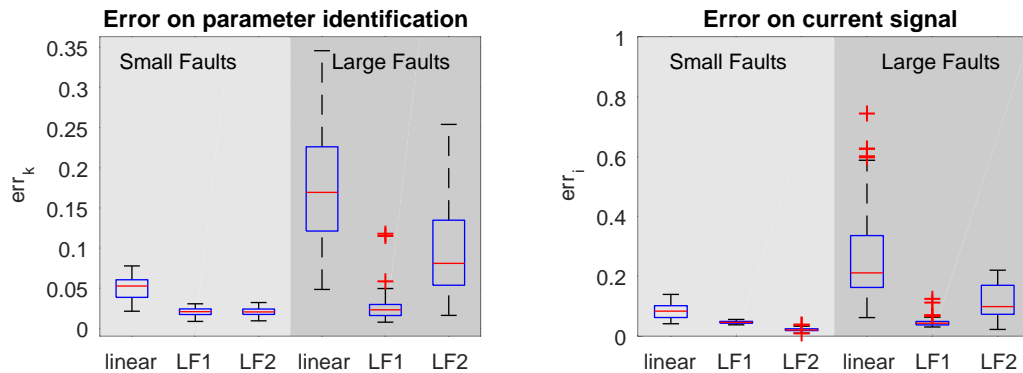


Figure 2: Relative errors in parameter identification (left) and output reconstruction (right) for different methods.

by evaluating the model with the faults estimated by the parameter identification. The error is computed as the L_2 norm of the residual between the reconstructed signal and the original signal \mathbf{i}_{ref} , normalized as follows:

$$err_i = \frac{\|\mathbf{i} - \mathbf{i}_{\text{ref}}\|}{\|\mathbf{i}_{\text{ref}}\|} \quad (6)$$

For all test cases the error on the signal reconstruction is coherent with the error on the identified parameters. The linearized approach works correctly for the test sets with limited faults, but it fails when the system is significantly far from the nominal condition.

Table 1: Computational times for the online parameter identification step

Test set	small faults			large faults		
Method	linear	LF1	LF2	linear	LF1	LF2
Computational time [s]	2.4e-4	1.8e1	1.6e0	1.9e-4	3.1e1	2.9e0

The iterative methods perform significantly better in the test sets characterized by a greater variation from the nominal conditions. In particular, the iterative approach exploiting the LF1 model shows the most consistent behavior in all the considered conditions, at the expense of a longer computational time (the fault identification takes in the order of tenths of seconds, Table 1). This method is then not suitable for hard real time applications, such as a continuous online fault estimation in flight.

The other iterative method, using the computationally lighter LF2 model, has intermediate performances between the linearized method and the first iterative method for the large damage condition, but takes significantly less computational time. Moreover, since the LF2 library is generated using the HF model, this signal emulator is able to reproduce the response of the HF model with higher accuracy than LF1 near the nominal condition, when the combined effect of multiple faults are negligible. This results in a slightly better accuracy of the second iterative method on the small faults test set, especially in terms of reconstruction error.

The computational cost of the QR factorization employed in the parameter estimation methods (see Section 3.2) increases with the cube of the matrix dimensionality. Then, the proposed signal compression strategy, lowering the amount of the data to process online of two orders of magnitude, results in a reduction of six orders of magnitude in the cost related to the QR factorization. This way, the considered methods for parameter estimation are applicable to the case study, most of the computational effort of the online phase being related to the execution of the models.

5 CONCLUSIONS

The paper discussed preliminary investigations conducted to assess the applicability of a sampling method, based on Proper Orthogonal Decomposition and Self-Organizing Maps, to the diagnostics of actuation system faults. The sampling technique is tested in combination with different methods for the resolution of a parameter estimation problem; the computational cost of the offline phase is mostly associated with the evaluation of the low fidelity model for the iterative methods, while the cost of the QR factorization is reduced of six orders of magnitude.

The results confirm that an in-flight fault detection is only viable with the linearized method, which can run in fractions of milliseconds and is more suitable for real-time executions of the algorithm. The method does not allow to identify the nature of fault modes causing the actuator current signal to diverge greatly from the nominal condition. However, the ability of detecting a small deviation from the nominal condition is enough to completely characterize the health status of the system when dealing with slowly growing faults, which are fairly common for electromechanical actuation systems. In addition, if the health status of the system is slowly evolving, the matrix $A(\mathbf{k})$ could be updated with a low frequency (e.g. every few flight hours, according to the rate of change of the estimated fault parameters) in order to perform the linearization near the last known fault condition \mathbf{k} . Conversely, since a hard real time fault detection is not always required in the considered situations, the iterative methods can be used to analyze a small section of time history of the system behavior (e.g. half a second of system response every few seconds to few minutes), to detect faults with a higher accuracy and robustness, possibly to integrate the information provided by the linearized method.

Further developments will be dedicated to reduce the computing time needed for the parameter estimation and increase the accuracy. Moreover, the task concerning RUL estimation will be investigated, for example by mapping in real time the system useful life directly from the reduced current signal to avoid a continuous fault identification. The information retained in the reduced signal could indeed allow for better results in RUL estimation than in fault identification, as observed for similar formulations adopted for real time structural assessment problems [7].

6 ACKNOWLEDGEMENTS

This work was supported by the Visiting Professor Program at Politecnico di Torino. The authors thank Prof. Paolo Maggiore at Politecnico di Torino for his support.

REFERENCES

- [1] Benedettini, O., Baines, T.S., Lightfoot, H.W. and Greenough, R.M. State-of-the-art in integrated vehicle health management. *Proceedings of the Institution of Mechanical Engineers Part G Journal of Aerospace Engineering* (2009) **223(2)**:157–170.
- [2] Williams, Z. Benefits of IVHM: an analytical approach. In: *2006 IEEE Aerospace Conference*, 4-11 March, Big Sky, MT, USA (2006)
- [3] Vachtsevanos, G., Lewis, F., Roemer, M., Hess, A. and Wu, B. *Intelligent fault diagnosis and prognosis for engineering systems* John Wiley & Sons, Inc., Hoboken, New Jersey (2006).
- [4] Lumley, J. The structure of inhomogeneous turbulent flows. *Atmospheric Turbulence and Radio Wave Propagation* edited by Yaglom, A. M., and Tatarsky, V. I., Nauka, Moscow (1967) 166–178.
- [5] Holmes, P.J., Lumley, J., Berkooz, G. *Turbulence, Coherent Structures, Dynamical Systems and Symmetry* Cambridge University Press (1996).
- [6] Walton, S., Hassan, O., and Morgan, K. Reduced order modelling for unsteady fluid flow using proper orthogonal decomposition and radial basis functions *Applied Mathematical Modelling* (2013) **37**:8930–8945.
- [7] Mainini, L. and Willcox, K.E. Sensor placement strategy to inform decisions. *18th AIAA/ISSMO Multidisciplinary Analysis and Optimization Conference, 2017 AIAA Aviation Forum*, 5-9 June, Denver, CO (2017).
- [8] Somervuo, P. and Kohonen, T. Self-organizing maps of symbol strings. *Neural Processing Letters* (1998) **12(1)**:19–30.
- [9] Somervuo, P. and Kohonen, T. Self-organizing maps and learning vector quantization for feature sequences. *Neural Processing Letters* (1999) **10(2)**:151–159.
- [10] Garcia Garriga, A., Govindaraju, P., Ponnusamy S.S., Cimmino N. and Mainini L. A modelling framework to support power architecture trade-off studies for More-Electric Aircraft. *Transportation Research Procedia* (2017) **29**:146–156.
- [11] Balaban, E., Saxena, A., Goebel, K., Byington, C.S., Watson, M., Bharadwaj, S., and Smith, M. Experimental Data Collection and Modeling for Nominal and Fault Conditions on Electro-Mechanical Actuators *Annual Conference of the Prognostics and Health Management Society*, 27 September–1 October, San Diego, CA (2009).
- [12] Berri, P.C., Dalla Vedova, M.D.L., and Maggiore, P. A smart electromechanical actuator monitor for new model-based prognostic algorithms. *International Journal of Mechanics and Control*. (2016) **17(2)**:59–66.

- [13] Bui-Thanh, T., Damodaran, M., and Willcox, K.E. Aerodynamic Data Reconstruction and Inverse Design Using Proper Orthogonal Decomposition. *AIAA Journal* (2004) **42(8)**:1505–1516.
- [14] Benner, P., Gugercin, S., Willcox, K. A survey of projection-based model reduction methods for parametric dynamical systems. *SIAM Review* (2015) **57(4)**:483–531.
- [15] Rathinam, M., Petzold, L.R., A new look at proper orthogonal Decomposition. *SIAM journal of numerical analysis* (2003) **41(5)**:1893–1925.
- [16] Amsallem, D. and Farhat, C. On the Stability of Reduced-Order Linearized Computational Fluid Dynamics Models Based on POD and Galerkin Projection: Descriptor vs Non-Descriptor Forms. In: *Reduced Order Methods for Modeling and Computational Reduction* edited by Quarteroni, A., Rozza, G. (2014) **9**:215–233.
- [17] Everson, R., Sirovich, L. The Karhunen-Loeve procedure for gappy data. *Journal of the Optical Society of America* (1995) **12(8)**:1657–1664.
- [18] Candes, E., Romberg, J., and Tao, T. Stable Signal Recovery from Incomplete and Inaccurate Measurements. *Communications on Pure and Applied Mathematics* (2006) **59(8)**:1207–1223.
- [19] Baraniuk, R.G., Cevher, V., Duarte, M.F., and Hedge, C. Model-Based Compressive Sensing. *IEEE Transactions on information theory* (2010) **56(4)**:1982–2001.
- [20] Donoho, D.L., Compressed Sensing. *IEEE Transactions on Information Theory* (2006) **52(4)**:1289–1306.
- [21] Mathelin, L., Pastur, L., Maitre, O.L., A compressed sensing approach for closed loop optimal control of nonlinear systems. *Theoretical and computational fluid dynamics* (2012) **26(1-4)**:319–337.
- [22] Zhang, Y., Theory of compressive sensing via l_1 -minimization: a Non-RIP analysis and extensions. *Journal of the Operations Research Society of China* (2013) **1(1)**:79–105.
- [23] Holmes, P.J., Lumley, J.L., Berkooz, G., Mattingly, J., and Wittenberg, R.W., Low-dimensional models of coherent structures in turbulence. *Physics Reports* (1997) **287**:337–384.
- [24] Sirovich, L., Turbulence and the dynamics of coherent structures. part 1: Coherent structures. *Quarterly of Applied Mathematics* (1987) **45**:561–571.
- [25] Willcox, K.E., Peraire, J. Balanced Model Reduction via the Proper Orthogonal Decomposition *AIAA journal* (2002) **40(11)**:2323–2330
- [26] Kohonen, T. *Self-Organizing Maps*, Springer-Verlag, New York, 3rd ed. (2001).